straction from other molecules besides I but mainly because the silicon-containing radicals produced by abstraction would undergo other secondary reactions. Radical addition reactions are important in these pyrolyses, as they were in the pyrolysis of allyltrimethylsilane,[1,2] but there are some quite subtle factors at play in determining the distribution of products from these reactions. This distribution depends not only on the balance between terminal and internal addition (terminal is favored), but also on whether a chain sequence can develop or not. As shown in Scheme IV, the latter factor could explain why there is more dimethylvinylsilane than trimethylvinylsilane, but more allyltrimethylsilane than allyldimethylsilane, in the pyrolysis of I. Application of similar arguments to the pyrolysis of II–IV leads to the conclusions in Table III, which summarizes the expected outcome of radical addition reactions.

Pyrolysis of II is simpler than I. Not only is there no retroene reaction, but also the $^{\bullet}CH_2SiMe_3$ radicals do not isomerize. Furthermore, there are no longer two abstraction routes; the only abstraction products besides Me_4Si would be 1,3-butadiene and $Me_3Si^{\bullet}$ radicals. Allyltrimethylsilane is the main silicon-containing addition product, being the only product from addition of $^{\bullet}CH_2SiMe_3$ radicals and also the product from the favored terminal addition of $Me_3Si^{\bullet}$ radicals (Table III).

The retroene reaction is more important in the pyrolysis of III and IV than in I, giving rise to the greater thermal lability of these compounds (Table I) and forming propene and the prominent silicon-containing products dimethylvinylsilane and trimethylvinylsilane, respectively (Table II). Ethene results from both homolysis and radical addition. Hydrogen abstraction from III, as from I, leads to an endo-cyclization product.

The effect of added methyl chloride on product composition is consistent with the foregoing ideas. The metathesis reaction between organosilyl radicals and methyl chloride essentially converts the former into methyl radicals; accordingly, products attributable to methyl radical reactions increased, while those attributable to organosilyl radical reactions decreased. In the pyrolysis of III and IV, formation of dimethylvinylsilane and trimethylvinylsilane was unaffected, confirming that these are products of retroene reactions (Scheme I).

Experimental Section

Compounds I–IV were generous gifts from Professor T. J. Barton of Iowa State University, who also gave us calibration samples of the vinylsilanes and the dimethylsilacyclohexene; the dimethylsilacyclopentene was a gift from Dr. G. Manuel of the University Paul Sabatier, Toulouse, France. Other silicon compounds were obtained commercially, as were the hydrocarbons.

Gas kinetic experiments were carried out in the improved LPP and SFR apparatus, as previously described.[13] Most of the SFR measurements were made with a 1.5-m column packed with 80–100 mesh Chromosorb 101 with a flow rate of 60 cm^3 min^{-1}, temperature programmed between 50 and 210 °C; a 2.5-m column packed with 10% SE-30 on 100–120 mesh diatomite was also used for some of the least volatile products. Retention times are listed in Table II. The same columns were used in the static pyrolysis apparatus attached to a GC/mass spectrometer, on which identification of every product was verified.

Acknowledgment. We are most grateful to Professor T. J. Barton for gifts of compounds and for his encouraging interest in this work. We are also grateful to Dr. G. Manuel, to Dr. G. Eaton for GC/mass spectrometry, and to the SERC for financial support.

Registry No. I, 18163-02-5; II, 763-13-3; III, 33932-65-9; IV, 763-21-3; C_2H_4, 74-85-1; C_3H_6, 115-07-1; C_4H_8, 106-98-9; Me_3SiH, 993-07-7; Me_4Si, 75-76-3; $HMe_2SiCH{:}CH_2$, 18243-27-1; $Me_3SiCH{:}CH_2$, 754-05-2; $HMe_2CH_2CH{:}CH_2$, 3937-30-2; $Me_3SiCH_2CH{:}CH_2$, 762-72-1.

(13) Davidson, I. M. T.; Dean, C. E. *Organometallics*, in press.

Steric and Electronic Factors Influencing Transition-Metal–Phosphorus(III) Bonding[1]

Md. Matiur Rahman, Hong Ye Liu, Alfred Prock,* and Warren P. Giering*

Department of Chemistry, Boston University, Boston, Massachusetts 02215

Received March 27, 1986

Literature data for the heats of reaction of phosphorus(III) compounds with $(\eta\text{-}C_5H_7NiMe)_2$, $MePt(PPhMe_2)_2(THF)^+$, and $\eta\text{-}CH_3C_6H_5Mo(CO)_3$ have been quantified in terms of σ-electronic (pK_a values of R_3PH^+), π-electronic ($E_{\pi a}$ values), and steric (cone angle, θ) properties of the ligands. The heats of reaction are linear functions of pKa, $E_{\pi a}$ (after the π-electronic threshold, π_t), and θ (after the steric threshold). π_t is a metal property and provides a ranking of the valence orbital energies of the various metals. Steric effects are important for all the reported heats of reaction for the formation of the octahedral complexes $L_3Mo(CO)_3$ but are not important for $\eta\text{-}C_5H_7Ni(Me)L$. The formation of $MePt(PPhMe_2)_2L^+$ exhibits steric efects only for the larger class II and class III ligands. Steric factors are more important for the class III (π-acid) ligands, which show a smaller steric threshold, than for the class II (σ-donor) ligands. The extension of these concepts to the dissociation of CO from *mer*-$(CO)_3LRu(SiCl_3)_2$ shows that steric acceleration of this reaction, which occurs in two narrow regions (steric windows), is determined by a combination of ground-state and transition-state steric effects.

Introduction

The development of a detailed understanding of the transition-metal–phosphorus bond is a problem that has been attacked by an impressive arsenal of techniques including theoretical calculations,[2,3] IR,[2c,d,4] NMR,[5]

(1) Second in a series of papers on the Quantitative Analysis of Ligand Effects (QALE). Previous paper: Golovin, M. N.; Rahman, Md. M.; Belmonte, J. E.; Giering, W. P. *Organometallics* **1985**, *4*, 1981–91.

(2) (a) Marynick, D. S. *J. Am. Chem. Soc.* **1984**, *106*, 4064–65. (b) Whango, M. H.; Steward, K. R. *Inorg. Chem.* **1982**, *21*, 1720–1. (c) Xiaxo, S.; Trogler, W. C.; Ellis, D. C.; Berkovitch-Yellin, Z. *J. Am. Chem. Soc.* **1983**, *105*, 7033–37.

0276-7333/87/2306-0650$01.50/0

Mössbauer,[6] UV/vis,[3] and photoelectron[7] spectroscopy, X-ray crystallography,[8] and electrochemistry.[9] Despite this effort, the separation of the σ, π, and steric components of the transition-metal–phosphorus bond has remained elusive.

The nature of the transition-metal–phosphorus bond is most directly probed by the analyses of metal–phosphorus bond energies. Unfortunately, there are few reports of the heats of addition (or substitution) of phosphorus(III) ligands to organometallic compounds.[10] In these studies, the heats of reaction were correlated with steric (cone angle, θ[11]) and electronic (ν or χ values[11]) properties of the ligands. The results of these analyses, which are claimed to show a major dependence of the heats of reaction on steric factors, however, provide little insight into the nature of the metal–phosphorus bond. Herein, we describe our analyses of the data from three of these papers[10a-c] by using our recently reported method, quantitative analysis of ligand effects (QALE).[1] The combined results of our analyses provide a remarkable insight into this chemical bond.

We begin with a brief overview of the electronic properties of phosphorus(III) ligands and then describe our method of analysis. This is followed by an examination of the heats of the three reactions. Finally, the concepts developed from these analyses are extended with fruitful results to the kinetics of dissociation of carbon monoxide from $(CO)_3LRu(SiCl_3)_2$.

Table I. Compilation of Ligand Properties of Phosphorus(III) Compounds

	ligand	θ[a], deg	pK_a[b]	$E_{\pi a}$[c]	$E_{\pi b}$[c]
1	$P(OCH_2)_3Et$	101	1.74	0.25[d,g]	
2	$PPhH_2$	101	(−2.0)		
3	$P(OMe)_3$	107	2.60	0.19[d,g]	
4	$P(OEt)_3$	109	3.31[e]	0.155[d]	
5	$P(OBu)_3$[f]	109	(3.31)	(0.155)	
6	PMe_3	118	8.65		
7	$PPh(OMe)_2$	120	(2.64)		
8	$PPhMe_2$	122	6.50		
9	PCl_3	124			
10	$P(OPh)_3$	128	−2.0[e]	0.25	
11	$P(O\text{-}p\text{-}ClC_6H_4)_3$	128			
12	$P(O\text{-}i\text{-}Pr)_3$	130	4.08[e]	0.14	
13	$PPhCl_2$	131			
14	$P(CH_2CH_2CN)_3$	132	1.36	0.16[g]	
15	PEt_3	132	8.69		0.004
16	PBu_3	132	8.43		0.027
17	$P(CH_2CHCH_2)_3$	132			
18	$PPh_2(OMe)$	132	(2.69)	0.11	
19	$PPh(OPh)_2$	134	(−0.4)	(0.193)	
20	$PPhEt_2$	136	6.25		
21	PPh_2Me	136	4.57		
22	PPh_2Cl	137			
23	$PPh_2(OPh)$	139	(1.15)	(0.129)	
24	PPh_2Et	140	4.9		
25	$P(O\text{-menth})_3$	140	(3.7)	0.109	
26	$P(O\text{-}o\text{-}MeC_6H_4)_3$	141	−1.83[e]	0.24	
27	$PPh(O\text{-menth})_2$	142	(4.2)	0.099	
28	PPh_3	145	2.73	0.069	
29	$P(p\text{-}MeC_6H_4)_3$	145	3.84		
30	$P(p\text{-}MeOC_6H_4)_3$	145	4.59		
31	$P(p\text{-}ClC_6H_4)_3$	145	1.03		
32	$P(p\text{-}FC_6H_4)_3$	145	1.97		
33	$P(O\text{-}o\text{-}i\text{-}PrC_6H_4)_3$	148	(−1.7)	0.24	
34	$PPh_2\text{-}i\text{-}Pr$	151			
35	$P(O\text{-}o\text{-}PhC_6H_4)_3$	152	(−2.0)	0.24	
36	PBz_3	165	(6.0)		
37	$P(m\text{-}MeC_6H_4)_3$	165	3.3		
38	$P(m\text{-}ClC_6H_4)_3$	165	(1.03)		
39	$P(c\text{-}C_6H_{11})_3$	170	9.7		0.07
40	$PPh_2(o\text{-}MeOC_6H_4)$	171			
41	$P(O\text{-}t\text{-}Bu)_3$	172	(4.5)	0.082	
42	$P(O\text{-}o\text{-}t\text{-}BuC_6H_4)_3$	175	(−1.0)	0.258	
43	$P(t\text{-}Bu)_3$	182	11.4		
44	$P(O\text{-}2,6\text{-}Me_2C_6H_4)_3$	190	(−0.4)	(0.24)	
45	$P(o\text{-}MeC_6H_4)_3$	194	3.08		

[a] Cone angle data were taken from ref 11 or estimated from information provided therein. [b] pK_a values for PR_3H^+ are taken from ref 12–14. Other pK_a values (in parentheses) were estimated on the basis of additivity plots if the pK_a values of other members of the homologous series are known, correlation with Hammett[15] σ or Kabachnik[16] σ^{Ph} constants or by comparison to phosphorus(III) compounds of similar structure. [c] Data taken from ref 1 except where noted. [d] New data based on recent measurements in our laboratories. [e] New pK_a value determined by the method of Streuli[17] using anhydrous nitromethane and trifluoromethane sulfonic acid. [f] The ligand properties of $P(OEt)_3$ were used as an estimate of the properties of this ligand. [g] A number of the $E_{\pi a}$ values reported in this table were determined by analysis of the new set of Tolman's ν values recently reported by Bartik.[4a] The analysis shows that the ν values of the class III ligands are related to the pK_a values and $E_{\pi a}$ values by the following equation: $\nu = -0.52(pK_a) + 95.7(E_{\pi a}) + 2063.8$. The small dependence of the ν values on the pK_a values of the ligands means that rather accurate $E_{\pi a}$ values can be obtained even for ligands for which we only have estimated pK_a values.

Classification of Ligands

About two and a half years ago while exploring ligand effects as a probe of the origin of the dramatic redox enhancement of certain organometallic reactions, we observed that the oxidation potentials of a series of manganese complexes $(\eta\text{-}MeC_5H_4)Mn(CO)_2L$ are related linearly to the Brønsted basicities (pK_a values of R_3PH^+) of certain

(3) Cotton, F. A.; Edwards, W. T.; Rauch, F. C.; Graham, M. A.; Perutz, R. N.; Turner, J. J. *J. Coord. Chem.* **1973**, *2*, 247–250.

(4) (a) Bartik, T.; Himmler, T.; Schulte, H.-G.; Seevogel, K. *J. Organometal. Chem.* **1984**, *272*, 29–41. (b) Tolman, C. A. *J. Am. Chem. Soc.* **1970**, *92*, 2953. (c) Goel, R. G.; Henry, W. P.; Srivastava, R. C. *Inorg. Chem.* **1981**, *20*, 1727–31. (d) Gray, G. M.; Kraihanzel, C. S. *J. Organometal. Chem.* **1983**, *241*, 201–214. (e) Graham, W. A. G. *Inorg. Chem.* **1968**, *7*, 315–21. (f) Stewart, R. P.; Treichel, P. M. *Inorg. Chem.* **1968**, *7*, 1942–44. (g) Albright, J. O.; Tanzella, F. L.; Verkade, J. G. *J. Coord. Chem.* **1976**, *6*, 225–29.

(5) (a) Bodner, G. M.; Gagnon, C.; Whittern, D. N. *J. Organomet. Chem.* **1983**, *243*, 305–14. (b) Bodner, G. M.; May, M. P.; McKinney, L. E. *Inorg. Chem.* **1980**, *19*, 1951–58. (c) Bodner, G. M. *Inorg. Chem.* **1975**, *14*, 2694–99. (d) Bodner, G. M. *Inorg. Chem.* **1974**, *13*, 2563–66. (e) Bodner, G. M.; Todd, L. J. *Inorg. Chem.* **1974**, *13*, 1335–38. (f) Bodner, G. M. *Inorg. Chem.* **1975**, *14*, 1932–35. (g) Grim, S. O.; Singer, R. M. *J. Coord. Chem.* **1978**, *8*, 121–26. (h) Masters, A. F.; Bossard, G. E.; George, T. A.; Brownlee, R. T. C.; O'Connor, M. J.; Wedd, A. G. *Inorg. Chem.* **1983**, *22*, 908–11.

(6) Johnson, B. V.; Steinmetz, A. L.; Ouseph, P. J. *J. Coord. Chem.* **1985**, *14*, 103–6.

(7) Bursten, B. E.; Darenbourg, D. J.; Kellog, G. E.; Lichtenberger, D. L. *Inorg. Chem.* **1984**, *23*, 4361–65.

(8) (a) Wovkulich, M. J.; Atwood, J. L.; Canada, L.; Atwood, J. D. *Organometallics* **1985**, *4*, 867. (b) Cotton, F. A.; Darensbourg, D. J.; Ilsley, W. A. *Inorg. Chem.* **1981**, *20*, 578–83. (c) Orpen, A. G.; Connelly, N. G. *J. Chem. Soc., Chem. Commun.* **1985**, 1310–11.

(9) Bond, A. M.; Carr, S. W.; Colton, R.; Kelly, D. P. *Inorg. Chem.* **1983**, *22*, 989–93.

(10) (a) Schenkluhn, H.; Scheidt, W.; Weimann, B.; Zahres, M. *Angew. Chem., Int. Ed. Engl.* **1979**, *18*, 401–2. (b) Manzer, L. E.; Tolman, C. A. *J. Am. Chem. Soc.* **1975**, *97*, 1955–6. (c) Nolan, S. P.; Hoff, C. D. *J. Organomet. Chem.* **1985**, *290*, 365–73. (d) Tolman, C. A.; Reutter, C. D.; Seidel, W. C. *J. Organomet. Chem.* **1976**, *117*, C30.

(11) Tolman, C. A. *Chem. Rev.* **1977**, *77*, 313. ν is the value (cm^{-1}) of the A_1 terminal carbonyl stretching frequency of $Ni(CO)_3$. χ is the difference between ν and the ν value (2056.1 cm^{-1}) for $P(t\text{-}Bu)_3$.

(12) Henderson, W. A.; Streuli, C. A. *J. Am. Chem. Soc.* **1960**, *82*, 5791–94.

(13) Allman, T.; Goel, R. G. *Can. J. Chem.* **1982**, *60*, 716–22.

(14) Jackson, R. A.; Kanluen, R.; Poe, A. *Inorg. Chem.* **1984**, *23*, 523–7.

(15) Hansch, C. H.; Leo, A. *Substituent Constants for Correlation Analysis in Chemistry and Biology*; Wiley: New York, 1980.

(16) Mastryukova, T. A.; Kabachnik, M. I. *Russian Chem. Rev.* (*Engl. Transl.*) **1969**, *38*, 795–811.

(17) Streuli, C. A. *Anal. Chem.* **1959**, *31*, 1652–54.

(18) Independently, Poe has also concluded that log k's for entering ligand dependent substitution reactions are linearly dependent on the pK_a values and cone angles of the entering phosphorus(III) ligands after the steric threshold. Personal communication.

ancillary triaryl and mixed aryl/alkyl phosphine ligands.[1] Complexes containing less basic and putative strong π-acid phosphorus(III) ligands were more difficult to oxidize than predicted by their basicities whereas the highly electron rich trialkylphosphines (π-bases) were more easily oxidized. The deviations of the formal reduction potentials from those predicted by the pK_a values are defined as $E_{\pi a}$ (π-acids) and $E_{\pi b}$ (π-bases). We suggested that these electrochemical parameters may be a good measure of the π-interaction between a phosphorus(III) ligand and a transition metal.[1]

On the basis of the above experimental observations the phosphorus(III) ligands are divided into three classes:

class I	σ-donor/π-donor
class II	σ-donor
class III	σ-donor/π-acceptor

The π-interactions between the metals and class III ligands are thought to be attractive and may involve metal valence d orbitals and phosphorus σ^* orbitals of appropriate symmetry.[2] We suggested previously that the π-interactions between metals and the class I ligands, which may involve filled metal valence orbitals and phosphorus σ-orbitals, appear to be generally repulsive in nature (vide infra).[1] Of particular importance is the observation that the onset of steric ligand effects occurs abruptly (steric threshold) when the size of the ligand exceeds that of the coordination site.[1] The ligands and their properties used in this study are presented in Table I.

Method of Analysis of the Heats of Organometallic Reactions

Our protocol for the analysis of heats of reaction data is presented briefly in this section. The analysis is based on the following assumptions that are applied to each set of reactions. (1) The heats of reaction are separable into terms that describe the σ-electronic (ΔH_σ and σ-steric (ΔH_σ^{st}) contributions as well as the π-electronic (ΔH_π) and π-steric (ΔH_π^{st}) contributions (eq 1). (2) The σ- and π-

$$\Delta H_{RX} = \Delta H_\sigma + \Delta H_\sigma^{st} + \Delta H_\pi + \Delta H_\pi^{st} \quad (1)$$

electronic contributions are linear functions of the pK_a values of PR_3H^+ and $E_{\pi a}$ (or $E_{\pi b}$), respectively, before and after the steric thresholds:

$$-\Delta H_\sigma = a(pK_a) + c \quad (2)$$

$$-\Delta H_\pi = b(E_{\pi a}) + c' \quad (3)$$

(3) The heats of reaction exhibit the same pK_a dependence regardless of the classification of the ligand and the involvement of steric effects. (4) The heats of reaction are linear functions of cone angle (θ) as well as pK_a values (and $E_{\pi a}$ or $E_{\pi b}$ values if appropriate) after the steric thresholds.[18]

It is tempting to use linear regression analysis in three parameters to separate the σ, π, and steric dependence of the data. This is, however, inappropriate because the data are not continuous functions of the three parameters (vide infra); there are distinct thresholds for the onset of steric and π-electronic effects. For detection of these thresholds, the preliminary analysis if performed graphically. If this is not possible (because of lack of appropriate data), then linear regression analysis is employed iteratively until a self-consistent set of results is obtained.

If steric effects are not important, the coefficient of the pK_a term of eq 2 is readily determined from the slope of the linear plot of data for the class II ligands vs. pK_a values

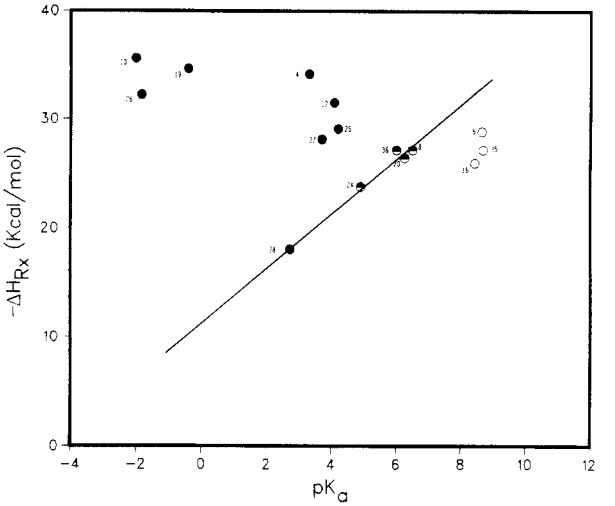

Figure 1. σ-Electronic profile for reaction 5. The slope of the line is taken from eq 8. Thermodynamic data are taken from ref 10a. Numbers refer to the ligands listed in Table I. ○ = class I ligands, ◓ = class II ligands, and ● = class III ligands. These symbols are used in the remaining figures where it is appropriate. The designation of the classification of a ligand is determined by its $E_{\pi a}$ value relative to the π_t of the metal.

(σ-electronic profile). This analysis requires that the ligands span a good range of pK_a values. We have found that most mixed phenyl/alkyl ligands behave consistently as class II ligands but that the extreme ends of this group may behave as class III (PPh_3) or class I ($PPhEt_2$ and PMe_3) ligands depending on the nature of the metal complex (vide infra). As steric factors become important, the data for the larger class II ligands will deviate from the σ-electronic profile. A plot of these deviations (ΔH_σ^{st}) vs. θ generates the σ-steric profile. If steric effects are important for all the class II ligands, then linear regression analysis (two parameter) is employed according to eq 4.

$$-\Delta H_{RX}(\text{class II}) = -\Delta H_\sigma - \Delta H_\sigma^{st} = a(pK_a) + d(\theta) + c' \quad (4)$$

The deviations of the class I and class III ligands from the σ-electronic (or steric) profile are attributed to π-electronic (ΔH_π) and π-steric (ΔH_π^{st}) effects. If there are no steric effects coupled with the π-electronic effects, then ΔH_π will correlate linearly with the $E_{\pi a}$ (or $E_{\pi b}$) values of the ligands (π-electronic profile). The $E_{\pi a}$ (or $E_{\pi b}$) intercept of the π-electronic profile is defined as the π-electronic threshold (π_t) (see Figures 2 and 5). The significance of π_t is described in the Discussion.

If steric factors are important, then the large class III ligands may deviate from the π-electronic profile. The plot of these deviations (ΔH_π^{st}) vs. θ gives the π-steric profile. Linear regression analysis is employed if steric effects appear to be operative for all ligands.

The analysis of the heats of reaction 5 illustrates our procedure. The heats of reaction for all ligands are plotted vs. their pK_a values in Figure 1. (All heats of reaction data are given in kilocalories per mole.) The putative class II

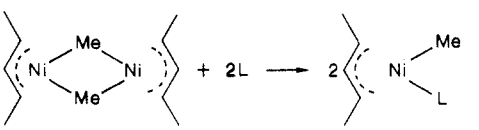

(5)

ligands (including PPh_3) appear to fall on a line that separates the class I ligands (points below the line) from the class III ligands (points above the line). Linear regression analysis of the data for the class II ligands gives

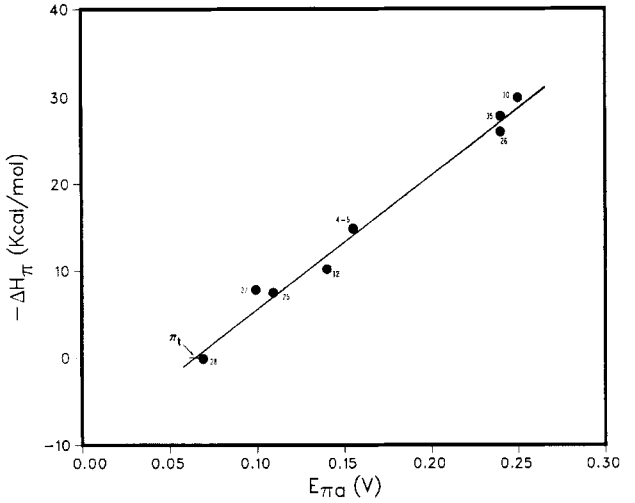

Figure 2. π-Electronic profile for the class III ligands of reaction 5. π_t is the π-electronic threshold; only phosphorus(III) ligands with $E_{\pi a}$ values greater than π_t behave as π-acids.

the following expression relating the heats of reaction to the pK_a values of these ligands:

$$-\Delta H_{RX}(\text{class II}) = -\Delta H_\sigma = 2.47(pK_a) + 11.37 \quad (6)$$

standard deviation = 0.50; r = 0.99

A plot of the deviations (ΔH_π) of the class III ligands from the line defined by eq 6 vs. the corresponding $E_{\pi a}$ values is also linear (standard deviation = 0.82; r = 0.995). The $E_{\pi a}$ intercept (π_t), however, is 0.053 V, thereby indicating that PPh_3 ($E_{\pi a}$ = 0.069 V) is behaving as a very weak π-acid ligand toward the nickel and should be included among the class III ligands. The removal of PPh_3 from the class II ligands leaves only four class II ligands which are too closely clustered in a narrow pK_a range (4.9–6.5) to be confidently analyzed. In view of this problem, the data for the class III ligands were then analyzed (two parameter linear regression analysis) with the inclusion of PPh_3 as one of these ligands (eq 7).

$$-\Delta H_{RX} = -\Delta H_\sigma - \Delta H_\pi = 2.58(pK_a) + 153.9(E_{\pi a}) + 1.23 \quad (7)$$

standard deviation = 1.16; r = 0.97

The pK_a dependence shown in eq 7 is virtually the same as that obtained when PPh_3 is treated as a class II ligand which is consonant with the borderline behavior of this ligand. The σ-electronic profile shown in Figure 1 was obtained by fitting the best line with a slope of 2.58 (from eq 7) to the points for the remaining four class II ligands. This is shown as eq 8. A plot of the deviations (ΔH_π) of

$$-\Delta H_\sigma = 2.58(pK_a) + 10.8 \quad (8)$$

the class III ligands from the line defined by eq 8 gives the linear π-electronic profile (standard deviation = 1.19; r = 0.993) displayed in Figure 2. By combining the $E_{\pi a}$ intercept (π_t) from Figure 2 and eq 7 and 8, we get an expression (eq 9) for the heats of reaction of the class II and class III ligands. (λ is a switching function that "turns on" the π-effect when $E_{\pi a} > \pi_t$.)

$$-\Delta H_{RX} = -\Delta H_\sigma - \Delta H_\pi = 2.58(pK_a) + \lambda(153.9(E_{\pi a}) - 9.57) + 10.8 \quad (9)$$

$$\lambda = 0,\ E_{\pi a} < 0.062 \text{ V};\ \lambda = 1,\ E_{\pi a} > 0.062 \text{ V}$$

The available ligand property data are insufficient for an indepth analysis of the class I ligands. Qualitatively, it can be seen that the heats of reaction of these electron-rich ligands (including PMe_3) are smaller than those predicted by eq 8.

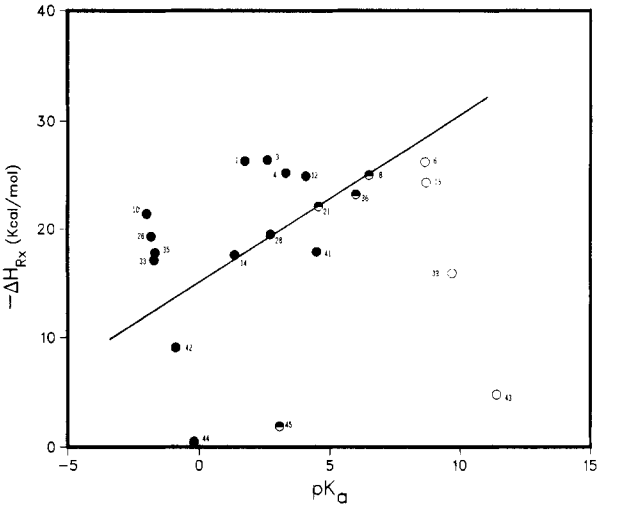

Figure 3. σ-Electronic profile for reaction 10. The slope of the σ-electronic profile, which is drawn through the small class II ligands, is taken from eq 11. Thermodynamic data are taken from ref 10b.

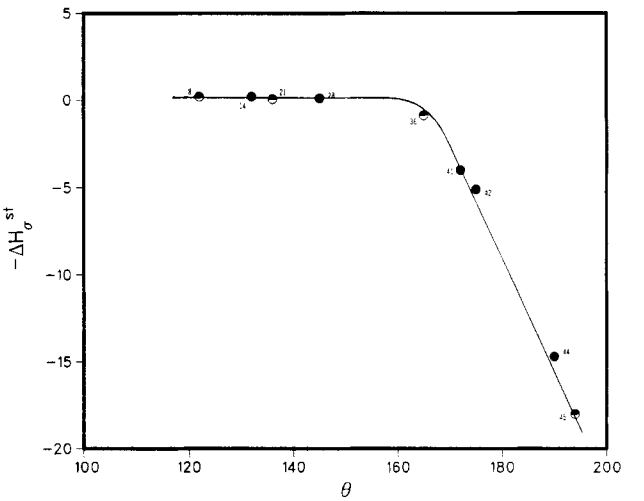

Figure 4. σ-Steric profile for reaction 10.

Extension of QALE to the heats of reaction 10 is straight forward although steric factors must be considered for the larger class II and class III ligands.[10b] Since only two small

$$MePtQ_2(THF)^+ + L \rightarrow MePtQ_2L^+ + THF \quad (10)$$

$$Q = PPhMe_2$$

mixed phenyl/alkyl phosphines (class II ligands) were employed in the study, the data for the five smallest (no steric contributions) class III ligands were treated by linear regression analysis (eq 11). When a line with a slope of

$$-\Delta H_{RX} = -\Delta H_\sigma - \Delta H_\pi = 1.43(pK_a) + 43.3(E_{\pi a}) + 13.51 \quad (11)$$

standard deviation = 0.435; r = 0.97

1.43 was passed through the points for the mixed phenyl/alkyl phosphines to generate the σ-electronic profile (Figure 3), the points for the moderately strong π-acid ligand $P(CH_2CH_2CN)_3$[19] and the weak π-acid ligand PPh_3

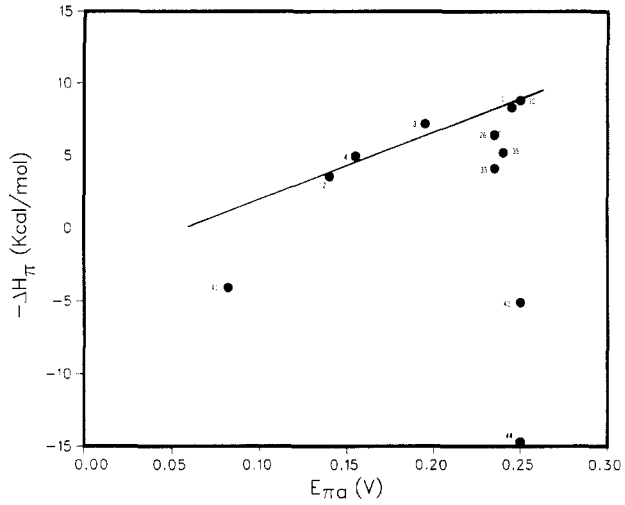

Figure 5. π-Electronic profile for reaction 10.

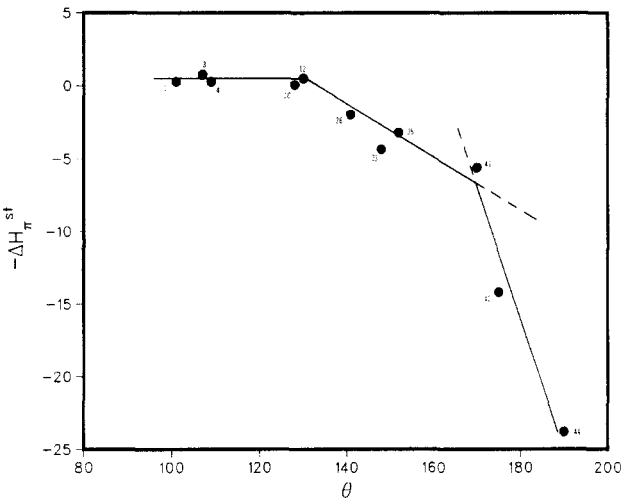

Figure 6. π-Steric profile for reaction 10.

are also observed to fall on or very close to the σ-electronic profile. Most of the remaining class III ligands lie above the line except for those with cone angles greater than 170°. The class I ligands, including PMe_3, lie below the line. The large class II ligands also exhibit heats of reaction smaller than those predicted by their pK_a values. The deviations (ΔH_σ^{st}) of the large class II ligands and the large class III ligands (vide infra) were used to generate the σ-steric profile (Figure 4) which shows a σ-steric threshold near 160°. The π-electronic profile (Figure 5) was generated by plotting the deviations ($\Delta H_\pi + \Delta H_\pi^{st}$) of the class III ligands from the σ-electronic profile in Figure 3 and then fitting a line with a slope of 43.3 (from eq 11) to these points. (Neither $P(CH_2CH_2CN)_3$ nor PPh_3 are included in the analysis at this point because of complicating steric factors (vide infra).) The resulting π-electronic profile shows a π_t value of 0.045 V. The π-steric profile (Figure 6) exhibits one steric threshold near 130° and another at 170° after which the profile descends more steeply. Equation 12 relates the heats of reaction for the small class II ($\theta < 160°$) and class III ($\theta < 130°$) ligands to their $E_{\pi a}$ and pK_a values.

$$-\Delta H_{RX} = -\Delta H_\sigma - \Delta H_\pi = 1.43(pK_a) + \lambda(43.2(E_{\pi a}) - 1.99) + 15.5 \quad (12)$$

$$\lambda = 0,\ E_{\pi a} < 0.045\ V;\ \lambda = 1,\ E_{\pi a} > 0.045\ V$$

(19) Cotton, F. A.; Darensbourg, D. J.; Ilsley, W. H. *Inorg. Chem.* **1981**, *20*, 578–583.

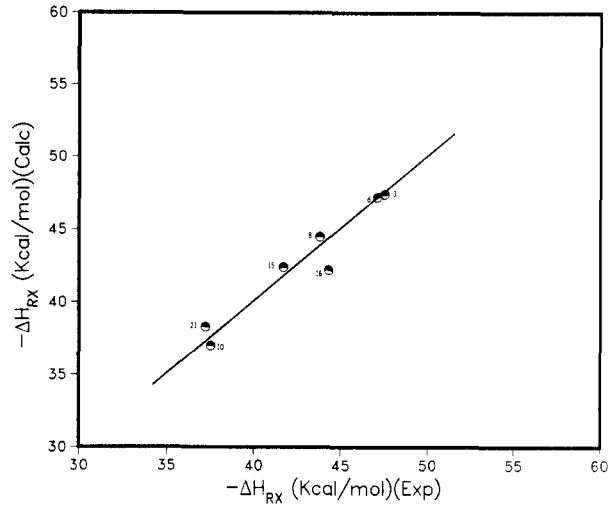

Figure 7. Comparison of the experimental heats of reaction 13 with those calculated by eq 14. Experimental data are taken from ref 10c. All ligands included in this analysis behave as class II ligands.

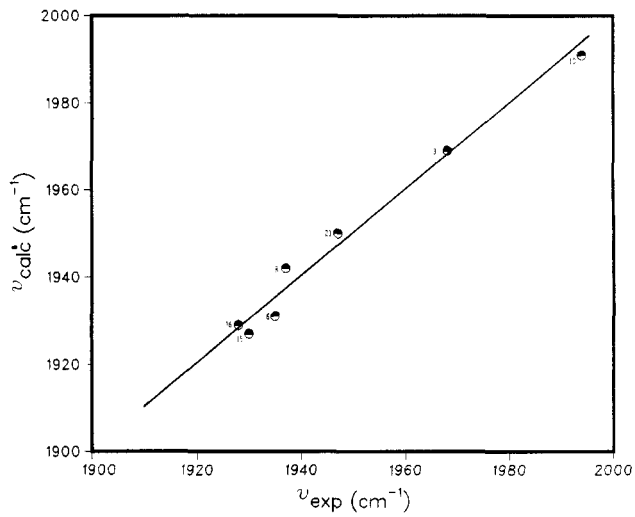

Figure 8. Comparison of the experimental A_1 terminal carbonyl stretching frequencies of $L_3Mo(CO)_3$ with those calculated by eq 15. Experimental data are taken from ref 10c. All ligands included in this analysis behave as class II ligands.

All class I ligands, including PMe_3, exhibit heats of reaction that are less than those predicted by their basicities.

Nolan and Hoff's[20] data for the heats of reaction 13 indicate that steric factors are operative for all ligands studied. Linear regression analyses of the heats of reaction and symmetric carbonyl stretching frequencies (ν_{A1} for $L_3Mo(CO)_3$) for all the ligands (classes I, II and III) show that these spectroscopic and thermodynamic properties are correlated only to the sizes and Brønsted basicities of the ligands.[21] The appropriate equations are shown below:

(20) Nolan and Hoff[10c] apparently experienced difficulty in obtaining the heat of reaction of PPh_3. We found that the datum for this ligand does not correlate well and therefore excluded it from the analysis. The excellent correlations between the experimental and calculated data shown in Figures 7 and 8 allow the "effective" pK_a value and cone angle of triphos ($Ph_2PCH_2CH_2P(Ph)CH_2CH_2PPh_2$) to be calculated by solving eq 14 and 15 using the reported heats of reaction and infrared data. The calculated effective pK_a value (5.53) is in agreement with the value (5.35) that is obtained when the "effective" pK_a of triphos is estimated assuming that it is simply an average of two PPh_2Et groups and one $PPhEt_2$ group. The calculated cone angle (130°) is similar to that for related diphosphines[11] (121–127°).

$$(MeC_6H_5)Mo(CO)_3 + 3L \rightarrow L_3Mo(CO)_3 + MeC_6H_5 \quad (13)$$

$$-\Delta H_{RX} = -\Delta H_\sigma - \Delta H_\sigma^{st} = 0.629(pK_a) - 0.354\theta + 83.6 \quad (14)$$

standard deviation = 1.0; r = 0.97

$$\nu_{A1} = -5.89(pK_a) - 0.255\theta + 2111.8 \quad (15)$$

standard deviation = 3.3; r = 0.99

A comparison of the calculated and experimental heats of reaction and ν_{A1} values are displayed in Figures 7 and 8.

Discussion

The QALE method demonstrates that the heats of reactions 5, 10, and 13 are determined by a combination of σ, π, and steric factors. The parameters for each of these reactions are presented in Table II. Electronic and steric factors are discussed separately.

Electronic Effects. The pK_a dependencies of the entering ligand dependent substitution reactions have been associated with the degree of orbital overlap in the transition state of the reaction.[14] We extend this concept to heats of reaction; σ- and π-orbital overlap between metal and phosphorus in the ground state are also related to the coefficients of the pK_a and $E_{\pi a}$ terms in eq 2 and 3. It is, however, necessary to correct the coefficients for the number of phosphines that are added to the complexes; thus, the coefficients for reactions 5 and 13 have been divided by 2 and 3, respectively. We see that the σ-orbital overlap (a/n in Table II) increases in the following order: $Pt(II)^+ > Ni(II) \gg Mo(0)$.

The π-electronic profiles (Figures 2 and 5) provide important information about the π-component of these reactions. First, π-bonding is extremely important and may account for up to 88% (30 kcal/mol) of the heat of reaction 5 and 42% (9 kcal/mol) of reaction 10.[22] Secondly, the onset of π-bonding occurs rather suddenly when the $E_{\pi a}$ value of the ligand exceeds the π_t value. Ligands with $E_{\pi a}$ values below π_t do not act as π-acids; this is described by the switching function, λ, for the $E_{\pi a}$ terms in eq 9 and 12.

The observation of a threshold (π_t) for the onset of π-bonding indicates that this bonding will not occur unless the energy difference between the appropriate metal and phosphorus orbitals is smaller than a critical value. Consequently, π_t is a measure of the energy of the metal valence orbital. This concept can be readily understood by consideration of Figure 9 that describes the π-interactions between a phosphorus ligand and a metal; the energies of the phosphorus orbitals change, but the energy of the metal valence orbital is invariant. The metal–phosphorus σ-bond has been omitted for the sake of clarity. In Figure 9a, the metal orbital lies equidistant from the lowest lying phosphorus σ^* and highest σ-orbital of a class II ligand. Also shown is a bonding region bounded by the dotted lines within which the phosphorus orbitals must lie energetically in order to interact with the metal orbital. In Figure 9a, the phosphorus orbitals lie outside the bonding region, thus the metal–ligand linkage is comprised of only a σ-bond. In Figure 9b, the energies of the phosphorus orbitals are lower and the σ^* orbital lies within the bonding region; the phosphorus ligand now acts as a π-acid (class III) ligand.

(21) It is curious that according to eq 15 increasing θ decreases ν. This may be associated with a preferential weakening of the M–CO bond rather than a change in the CO bond strength.

(22) In our first paper[1] describing QALE we found that π-effects are not important in the reactions analyzed therein. This certainly is not the case with reactions 5 and 10.

Table II. σ, π, and Steric Parameters for Heats of Reactions 5, 10, and 13

reaction	$(a/n)^a$	$(b/n)^a$	$\pi_t{}^b$
5	1.29	77.0	0.062
10	1.43	43.3	0.045
13	0.209		
$MeC_5H_4Mn(CO)_2L$			0.0[c]

[a] Normalized coefficient that takes into account number (n) of reacting phosphines. Coefficient a is in units of kcal mol^{-1} while coefficient b is in units of kcal mol^{-1} V^{-1}. Coefficients are taken from eq 2 and 3. [b] π-Electronic threshold (in V)—a measure of the metal valence orbital energy and the π-acidity required of a ligand before metal-phosphorus back-bonding will occur. See Figures 2 and 5. [c] Standard on which $E_{\pi a}$ scale is based.

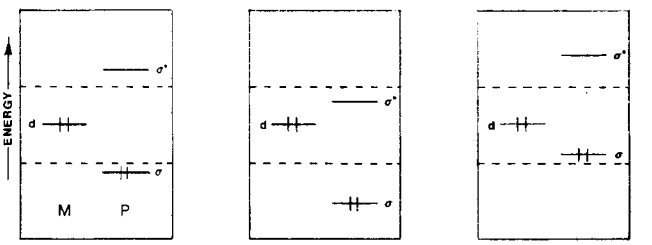

Figure 9. Phosphorus–metal π-orbital interaction diagrams illustrating the manner in which orbital energetics affect the classifications of the ligands and determined the π_t values of the metal. The σ-component of the metal–phosphorus bond has been omitted for the sake of clarity. M and P designate the metal and phosphorus orbitals, respectively.

In Figure 9c the phosphorus orbitals are at higher energy and the σ-orbital is within the bonding region; the ligand now acts as a π-base as is probably the case with the trialkylphosphines.

The classification of the ligands as class I, II, or III is dependent on the relative energies of the metal and phosphorus valence orbitals. Therefore, changes in the energies of the metal valence orbitals (by changing ancillary ligands, metals, and/or oxidation states) can also affect the classification of the ligands. Moving the metal orbital and the corresponding bonding region to sufficiently higher energy transforms the class II ligand of Figure 9a into a class III ligand; thus, because the metal orbital is at higher energy, the onset of π-bonding occurs with ligands of smaller $E_{\pi a}$ values, and a smaller π_t value is observed. On the other hand, moving the metal orbital to sufficiently lower energy will transform a class II ligand into a class I ligand, and some borderline class III ligands into class II ligands; in this situation only the stronger class III ligands will participate in π-bonding and a larger value of π_t will be observed.

Metals with π_t values greater than 0.0 V have valence orbital energies less than those of η-$MeC_5H_4Mn(CO)_2L$ (the complex on which the $E_{\pi a}$ scale is based), whereas those with π_t values less than 0.0 V will have valence orbital energies greater than the manganese complex. Thus, the valence orbital energy of the platinum is greater than that of the nickel, but both are less than that of the manganese. It is this decrease in metal valence orbital energy that accounts for the transformation of PMe_3 from a class II ligand for manganese to a class I ligand for the nickel and platinum.

Since the platinum has a higher valence orbital energy than nickel, it might be argued it should form the stronger π-bond to phosphorus(III) ligands. As can be seen from the preceding analysis, the metal valence orbital merely determines the ligand classification. It is orbital overlap that controls the "intrinsic" strength of the bond. We propose that the normalized coefficients (b/n of Table II)

of the $E_{\pi a}$ terms are a direct measure of the orbital overlap and, therefore, of the intrinsic metal–phosphorus bond strength. Thus, it can be seen that b/n for nickel is 1.75 times larger than that of platinum, consonant with the greater values of ΔH_π for the nickel complex.

Although we have not quantified the data for the class I ligands, inspection of Figures 1 and 3 for reactions 5 and 10, respectively, shows that the heats of reaction of these trialkyl ligands are less than those predicted by their basicities. This diminution of the heats of reaction cannot be attributed to steric factors since even the small ligand PMe_3 (θ = 118°) behaves in this manner; therefore, this observation supports our contention that there is a repulsive π-electronic interaction between metals and the class I phosphorus(III) ligands.

Steric Effects. While it is not necessary to invoke steric factors in the analysis of reaction 5, steric effects must be considered in the analysis of reaction 10. On the basis of only electronic considerations, $P(CH_2CH_2CN)_3$ and PPh_3, which have $E_{\pi a}$ values greater than the π_t value of the platinum, should behave as class III ligands; however both behave as class II ligands in reaction 10. The π-electronic profile (Figure 5) shows that other class III ligands with $\theta > 130°$ experience steric attenuation of π-bonding to the metal. This π-steric threshold at 130°, which is less than the σ-steric threshold (160°), is not unexpected since it is known that multiply bonded phosphorus ligands sit deeper in the coordination site[8a] and should experience more severe steric interactions than singly bonded ligands. The π-bond between PPh_3 and platinum should be approximately 2.0 kcal/mol on the basis of eq 12. ΔH_π is diminished sterically, however, by 3.0 kcal/mol at θ = 145° (Figure 6). Therefore, it appears that it is energetically advantageous for PPh_3 to sit farther out in the coordination site and behave as a class II ligand. (Recent electrochemical measurements in our laboratory suggest that the cone angle of $P(CH_2CH_2CN)_3$ is considerably larger than the 132° determined by the method of Tolman. This might account, in part, for the class II behavior of this ligand.) Thus, it appears that the π-bond is of relatively short range and eventually becomes completely attenuated as the phosphorus(III) ligand is forced sterically away from the metal center.

Either extreme steric requirements for the ligand and/or crowding about the metal center will make even strong class III ligands behave as class II ligands. In support of this hypothesis, it appears that the largest of the class III ligands in reaction 10 behave as class II ligands. This accounts for the second steric threshold in Figure 6. When the three ligands are analyzed as class II ligands, they fall on the σ-steric profile (Figure 4).

Further evidence for the steric transformation of class III ligands to class II ligands comes from the QALE analysis of reaction 13 which shows that the heats of reaction are dependent only on the Brønsted basicities and sizes of the ligands. Thus, the σ-steric threshold for the molybdenum complex is less than the cone angle (107°) of $P(OMe)_3$. The π-steric threshold must be considerably smaller. π-Effects are not important even for strong π-acids such as $P(OPh)_3$. Thus, π-bonding in this octahedral complex has been completely attenuated sterically.

Additional evidence pertaining to the steric attenuation of metal–phosphorus(III) π-bonding comes from analyses of entering ligand dependent substitution reactions. For example, Poe observed that log k's of reaction 16 are related linearly to the pK_a values of most of the entering phosphorus(III) ligands including many class III ligands.[14] This is in accord with our contention that at long metal-phosphorus distances, which seems likely in these reactions, there is only σ bonding. (The very large ligands were rather unreactive presumably because of steric inhibition of the reaction.) The ligand, $P(OCH_2)_3Et$, was unusual in that its reactivity was much larger than that predicted by its basicity. $P(OMe)_3$ is also slightly more reactive than expected. Similarly, in our analysis[1] of Basolo's data[23] for reaction 17 we found that the small ligand $PPhH_2$ is more

$$Me_2N_4Fe(CO)_3 + L \rightarrow Me_2N_4Fe(CO)_2L + CO \quad (17)$$

reactive than predicted by its basicity. All three of these ligands are small and are moderate to strong class III ligands. We propose that in certain cases these ligands can approach close enough to the metal in the transition state to experience both significant σ- and π-bonding.

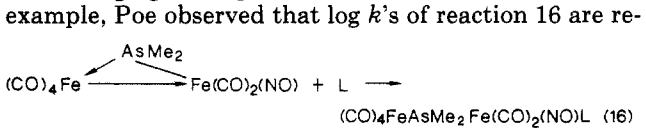

Comparison of QALE with Previous Analyses

It is instructive at this juncture to compare the original analyses of the data for reactions 5, 10, and 13 with those described herein. It will be seen that QALE analyses support and build on most of the earlier interpretations. Eq 18 (reaction 5) and 20 (reaction 13) were obtained by linear regression analysis by the original authors in terms of ν (or χ) values and cone angle. In a similar manner,

$$-\Delta H_{RX} = 1.65(\chi) - 0.56(\theta) + 172.0 \quad (18)$$

$$-\Delta H_{RX} = -0.0704(\nu) - 0.218(\theta) + 196.6 \quad (19)$$

$$-\Delta H_{RX} = -0.254(\nu) - 0.362(\theta) + 613.0 \quad (20)$$

we analyzed the data for reaction 10 (eq 19, r = 0.84). This poor correlation coefficient is attributed to the failure of this analysis to take into account the action of the σ- and π-steric thresholds. (See Figures 4 and 6.)

In order to compare the original analyses with the QALE analyses, we note there is a rough inverse relationship between the ν (or χ) values and ligand Brønsted basicities. In a similar sense there is a direct relationship between the π-acidities of the ligands and the ν and χ values.

Schenkluhn's analysis[10a] of reaction 5 (eq 18) shows that the heats of reaction increase as the χ values of the ligands increase and decrease as θ increases. This steric dependence is unexpected since $LNi(CO)_3$ fails to show a steric effect even for ligands with cone angles as large as 194°.[11] In order to obtain a reasonable correlation, it was necessary to exclude from consideration PPh_3, PBz_3, and PPh_2Et. (In general, these and other compounds bearing two or three phenyl groups, many of which are class II ligands, tend not to correlate well in these analyses.[24]) We reanalyzed the data, in terms of θ and ν, for the ten class III ligands including PPh_3 but excluding, as did Schlenkluhn et al., $PPh_2(OEt)$ because it appears to be anomalous. (The class I ligands were omitted because of the lack of appropriate ligand property data for the QALE analysis.) Linear regression analysis in terms of θ and χ values gave a correlation coefficient of 0.86; inclusion of the class II ligands gave even a poorer correlation. Analysis in terms of pK_a and $E_{\pi a}$ values gave a much better correlation (r = 0.94); deletion of the datum for $PPh(OPh)_2$, which also appears anomalous, raises the correlation coefficient to 0.974. We conclude, therefore, at least for the class II and class III ligands that steric factors are not playing an important role in reaction 5.

(23) Chang, C.-Y.; Johnson, C. E.; Richmond, T. G.; Chen, Y.-T.; Trogler, W. C.; Basolo, F. *Inorg. Chem.* **1981**, *20*, 3167–72.
(24) Schenkluhn, H.; Berger, R.; Pittel, B.; Zahres, M. *Transition Met. Chem. (Weinheim, Ger.)* **1981**, *6*, 277–87 and references therein.

The χ dependence of eq 18 is consistent with π-bonding dominating the nickel–phosphorus linkage. QALE analysis show that up to 88% of the heat of reaction 5 can be attributed to π-effects.

In their original analysis of the thermodynamic data, Manzer and Tolman[10b] concluded that the steric properties play the dominant role in the determination of the heats of reaction 10. Although their plot of heats of reaction vs. cone angle shows a definite trend toward lower heats of reaction with increasing cone angle, there was considerable scatter of the data. Two curves were actually drawn by them—one for the phosphite ligands and the other for the alkyl and aryl phosphines. It is noteworthy that the two sets of ligands appear to behave in a disparate manner at small cone angles and then with increasing similarity at larger cone angles. It was noted by the authors that an electronic effect was operative since the isosteric ligands $P(CH_2CH_2CN)_3$ and PEt_3 gave very different heats of reaction. No attempt was made to separate the electronic and steric factors. Linear regression analysis (in term of ν values and cone angle) of the data for reaction 10 (eq 19) shows that there is a small negative correlation with the ν values consistent with a slight dominance of σ-bonding. QALE analysis shows that both σ- and π-effects are important contributors to the heats of reaction; therefore any changes in σ-bonding because of changes in the Brønsted basicities are largely compensated for by changes in π-bonding. The net effect is that the correlation between the heats of reaction 10 and the ν values is largely erased leaving only steric effects readily observable. QALE also shows that the larger class III ligands (phosphites) function as class II ligands which accounts for the convergence of the two curves originally drawn by Manzer and Tolman.

Nolan and Hoff noted that the heats of reaction 13 increase (eq 20) as the ν values of the ligands decrease (basicities increase). Thus, their results are in agreement with our analysis which shows that the π component of the molybdenum–phosphorus bond is completely "turned off" sterically leaving only the σ-component operative.

Steric Attenuation of Metal–Phosphorus Bonding in the Dissociation of Carbon Monoxide from a Ruthenium Complex

The concept that the metal–phosphorus π-bond is attenuated sterically before the σ-bond helps to explain the rather strange steric profile that results from the QALE analysis of the kinetic data for reaction 21. In 1984, Chalk and Pomeroy reported the results of an extensive and well-designed study of ligand effects on the kinetics of substitution of carbon monoxide from the complex *mer*-$(CO)_3LRu(SiCl_3)_2$ (eq 21).[25]

$$(CO)_3LRu(SiCl_3)_2 + L' \rightarrow (CO)_2L'LRu(SiCl_3)_2 + CO \quad (21)$$

$$\text{rate} = k_{obsd}[\text{complex}]$$

The kinetic data were collected for a large variety of ligands (L) that spanned a broad range of pK_a values and cone angles. The reaction is first order in complex and independent of the concentration of the entering ligand (L'). A qualitative analysis[26] of the rate data for ligands

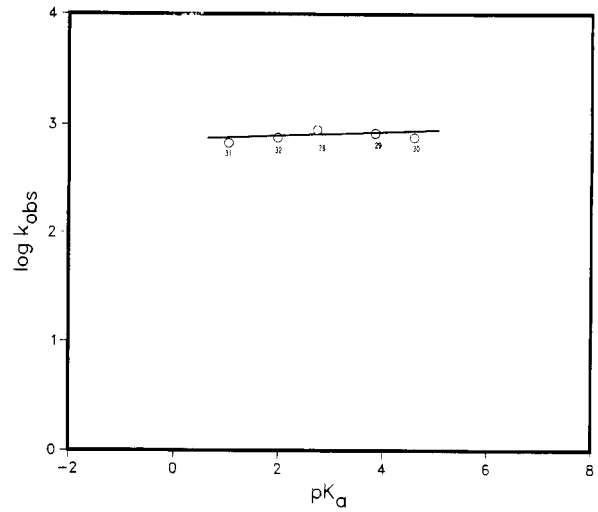

Figure 10. The σ-electronic profile of reaction 21. Kinetic data are taken from ref 26. No classification of the ligands is intended by the open circles.

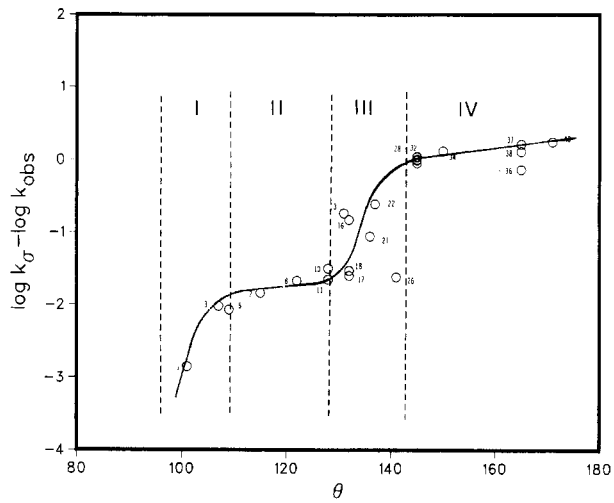

Figure 11. The steric profile of reaction 21. No classification of the ligands is intended by the open circles. The four regions bounded by the dotted lines are discussed in the text.

of similar cone angles suggested that electronic factors were not playing a significant role in the determination of the rates of reaction and that steric acceleration was the dominant force in the ligand effects.

Our interpretation of the QALE analysis for this set of ligands supports the conclusions of the original authors. The electronic profile (Figure 10) for the isosteric para-substituted triarylphosphines has a slight positive slope consistent with a small preferential transition-state electronic stabilization that is associated with the σ-donicity of the ligands. There is no evidence that π-effects are operative for these triaryl ligands. This almost insignificant electronic dependence allowed us to use data for ligands for which only roughly estimated pK_a values are available.

The steric profile (Figure 11) was generated by plotting the deviation of log k_{obsd} from that predicted by the electronic profile shown in Figure 10 vs. cone angle. This profile demonstrates that steric acceleration is not continuous but rather occurs in two narrow regions. The steric profile initially rises very rapidly below 110° and then

(25) Chalk, K. L.; Pomeroy, R. K. *Inorg. Chem.* **1984**, *23*, 444–49.

(26) A reviewer suggested that Tolman cone angles are inappropriate as a measure of size of phosphorus(III) ligands, thereby giving rise to the strange steric profile. Although there is some controversy surrounding the use of Tolman's cone angles,[27] we have found no systematic variations or other compelling evidence suggesting that Tolman's cone angles are not the best measure of ligand size. Until such evidence appears we feel obligated to use this set of cone angles and to interpret the results of the QALE analyses accordingly.

(27) (a) Clark, H. C. *Israel J. Chem.* **1976/1977**, *15*, 210–13. (b) DeSanto, J. T.; Mosbo, J. A.; Storhoff, B. N.; Bloss, R. E. *Inorg. Chem.* **1980**, *19*, 3086–92.

"plateaus" between 115° and 130°, after which it again rises rapidly before "plateauing" for a second time above 140°.

The shape of the steric profile suggests that steric destabilization is being observed not only in the ground state but also in the transition state of the reaction.[26] Analyses of structural[18] and kinetic data[1,18] suggest that there are specific volumes associated with the coordination sites of the species that are found along the potential energy surface of organometallic reactions. The site volume for the ancillary phosphorus(III) ligand in the transition state (reaction 21), which is on its way to being pentacoordinate, is larger than the site volume in the hexacoordinate ground state. When the size of the ancillary phosphorus ligand exceeds the site volume in either structure, there is abrupt destabilization. Since the transition state for reaction 21 is less congested than the ground state, it is obvious that the ground state must exhibit a smaller steric threshold than the transition state. Thus, the steric profile for this reaction will exhibit a region beginning at small cone angles where steric effects are not important. As the size of the ligand increases, there is a π-steric threshold that ushers in steric attenuation of the metal–phosphorus π-bond in the ground state and a second π-steric threshold that marks the beginning of steric effects in the transition state. (Roman numerals used in the remainder of this discussion refer to the regions designated in Figure 11.) Between these thresholds (π-steric window,[28] region I), the energy of the ground state rises more rapidly than that of the transition state. (The longer range σ-bond is not appreciably affected at this point.) In region I, the reaction shows a dramatic steric rate acceleration. After the π-steric thresholds the class III ligands are forced away from the metal and the π-bonding is diminished first in the ground state and then in the transition state until the ligand behaves only as a class II ligand. After the second π-steric threshold (region II) the transformation to a class II ligand is complete. Since the class II ligands sit farther out in the coordination site, their coordination site volume is larger. Therefore, there is no further significant destabilization of either the ground state or the transition state until the class II ligands exceed the size of the coordination site. There is then a plateau (region II) between the second π-steric threshold and the first σ-steric threshold. After the first σ-steric threshold, the ground-state energy again rises rapidly until the second σ-steric threshold, which marks the onset of steric destabilization of the transition state (region III). The energies of the ground and transition states then rise together so that the difference between the two states increases more slowly; hence, after the second σ-steric threshold the rates of reaction show only a small response to the steric size of the ancillary ligand (region IV). We have termed this phenomenon "steric saturation".

Steric saturation and the attendant steric windows add a new and important dimension to the design and analysis of ligand effect studies. The information that can be gleaned from such studies will lead to a detailed understanding of organometallic reaction mechanisms. For example, the width of the steric window can provide information on the relative structures of the transition state and ground state. If the steric window is narrow, the ground state and transition state are of similar structure. In contrast, a wide steric window indicates that the structures of the ground state and transition state are disparate. The significance of this and other steric parameters, such as steric sensitivity,[1] cannot be appreciated until a larger body of data for other related reactions becomes available.

(28) The term steric window was introduced recently. Cotton, J. D.; Markwell, R. D. *Organometallics* **1985**, *4*, 937–9.

Conclusions

The σ, π, and steric components of the transition-metal–phosphorus bond can be separated quantitatively by using QALE. There are distinct thresholds for the onset of metal–phosphorus π-bonding and steric effects. The onset of π-bonding occurs when the $E_{\pi a}$ value of the ligand exceeds, the π_t value of the metal, barring steric inhibition. This π_t value depends on the energy of the metal valence orbital and thereby provides a ranking of metal orbital energies. The π-bond is of shorter range than the phosphorus–metal σ-bond and is more susceptible to steric attenuation. It the steric requirements of the complex or the ligand become sufficiently demanding, then class III (π-acid) ligand apparently are forced away from the metal and in the extreme behave as class II ligands. The analysis of the dissociation of CO from *mer*-$(CO)_3RuL(SiCl_3)_2$ demonstrates that the interpretation of steric ligand effects must be done with caution and that the ligands used in the experiments must lie in a useful steric domain. Clearly, a detailed picture of the metal–phosphorus bond is emerging via QALE.

Registry No. **1**, 280-45-5; **2**, 638-21-1; **3**, 121-45-9; **4**, 122-52-1; **5**, 102-85-2; **6**, 594-09-2; **7**, 2946-61-4; **8**, 672-66-2; **9**, 7719-12-2; **10**, 101-02-0; **11**, 5679-61-8; **12**, 116-17-6; **13**, 644-97-3; **14**, 4023-53-4; **15**, 554-70-1; **16**, 998-40-3; **17**, 16523-89-0; **18**, 4020-99-9; **19**, 13410-61-2; **20**, 1605-53-4; **21**, 676-59-5; **22**, 1079-66-9; **23**, 13360-92-4; **24**, 607-01-2; **26**, 2622-08-4; **28**, 603-35-0; **29**, 1038-95-5; **30**, 855-38-9; **31**, 1159-54-2; **32**, 18437-78-0; **33**, 31502-35-9; **34**, 6372-40-3; **35**, 2752-19-4; **36**, 7650-89-7; **37**, 6224-63-1; **38**, 29949-85-7; **39**, 2622-14-2; **40**, 53111-20-9; **41**, 15205-62-6; **42**, 31502-36-0; **43**, 13716-12-6; **44**, 52830-49-6; **45**, 6163-58-2; $[(CH_3CHCH{=}CHCH_3)Ni(\mu\text{-}CH_3)]_2$, 68472-10-6; $MePt(PPhMe_2)_2(THF)^+$, 55280-16-5; $(MeC_6H_5)Mo(CO)_3$, 12083-34-0.